ACS APPLIED MATERIALS & INTERFACES

RESEARCH ARTICLE

www.acsami.org

Enhanced Field-Emission from SnO_2:$WO_{2.72}$ Nanowire Heterostructures

Deodatta R. Shinde,[†] Padmakar G. Chavan,[†] Shashwati Sen,[*,‡] Dilip S. Joag,[†] Mahendra A. More,[*,†] S. C. Gadkari,[‡] and S. K. Gupta[‡]

[†]Center for Advanced Studies in Materials Science and Condensed Matter Physics, Department of Physics, University of Pune, Pune 411007, India

[‡]Technical Physics Division, Bhabha Atomic Research Center, Mumbai −400085

ABSTRACT: The field-emission properties of SnO_2:$WO_{2.72}$ hierarchical nanowire heterostructure have been investigated. Nanoheterostructure consisting of SnO_2 nanowires as stem and $WO_{2.72}$ nanothorns as branches are synthesized in two steps by physical vapor deposition technique. Their field emission properties were recorded. A low turn-on field of ~0.82 V/μm (to draw an emission current density ~10 μA/cm^2) is achieved along with stable emission for 4 h duration. The emission characteristic shows the SnO_2:$WO_{2.72}$ nanoheterostructures are extremely suitable for field-emission applications.

KEYWORDS: SnO_2:$WO_{2.72}$ heterostructures, 1D nanostructures, field emission, (Vapor-Solid) VS process, interfaces

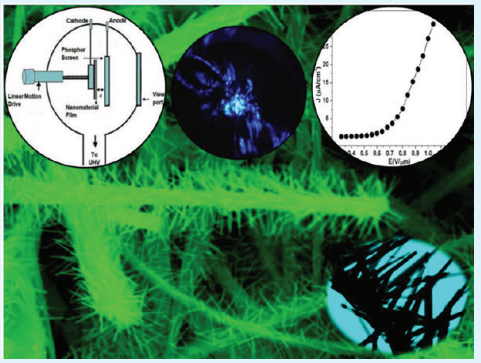

INTRODUCTION

The presence of various novel optical, electronic, and other properties have led to research in the field of nanostructures and their applications.[1,2] The assembly of one-dimensional (1D) nanostructures like nanowires and nanorods have application in the fabrication of nanoelectronic and nanophotonic devices. In particular, semiconductor and metal nanowires or nanorods are considered to be important building blocks in the fabrication of future nanodevices. The electrical, optical and mechanical properties of these 1D structures have been shown to be further modified by addition of a 1D structure of another material leading to the formation of a hierarchical nanoheterostructure.

The branched nanostructures constitute a unique class of materials where tiny nanowire branches grow on a larger nanowire stem of different functionality. Hierarchical heterostructures are useful for the realization of multicomponent functional nanodevices because the cores and branches of these nanostructures are composed of different materials. Also the aspect ratio and surface to volume ratio of these materials are extremely high. Several research groups have reported on their potential applications as interconnects, gas sensor, field emitters etc.[3−7] For a material to be used as a field emitter, the requirements are low threshold voltage, high emission current density, and good stability. To achieve low threshold field, the material should possess low work function and/or high field-enhancement factor (β). The field-enhancement factor in turn can be increased by increasing the aspect ratio of the material as in the case of one-dimensional nanostructures and heterostructures. Baek et al. have already reported the superior field-emission properties of nanoheterostructure of W nanothorn arrays on WO_3 nanowhiskers.[8]

Tungsten oxide (WO_3) is an important metal oxide semiconductor because of its robustness, chemical stability, and high melting point. Because of these properties WO_3 has gained popularity in field-emission applications.[9,10] Our group has also reported the field-emission properties of $WO_{2.72}$, which is a suboxide of WO_3.[11] Another important metal oxide semiconductor whose nanostructures have been extensively investigated is SnO_2. This material has been mainly studied for gas sensing applications. Our group has shown the field emission properties of RuO_2-doped SnO_2 (RuO_2:SnO_2) and In, Sb-doped SnO_2 wires, both as a bunch and as an isolated single wire.[12−14] Our work has shown that SnO_2 is an attractive material for field emission particularly for high current density applications. Some heterostructures of SnO_2 in combination with other oxide-semiconductors like ZnO have been recently reported.[15−18] However, the field emission properties of these heterostructures have not been investigated. In this communication we report our investigations on field emission properties of SnO_2:$WO_{2.72}$ nanoheterostructures. They consist of SnO_2 nanowires at the core (stem) and $WO_{2.72}$ nanothorns grown on them (branches). Both the materials are single crystalline in nature and are grown by vapor soild deposition technique. These nanoheterostructures exhibited admirable field emission characteristics, a low turn-on field (~0.82 V/μm) and stable emission current. Because of the

Received: September 5, 2011
Accepted: November 8, 2011
Published: November 08, 2011

 © 2011 American Chemical Society

unusual geometry of the emitter, the field-emission properties of the present heteronanostructures are superior to pure SnO_2, WO_3, and other nanoheterostructures.

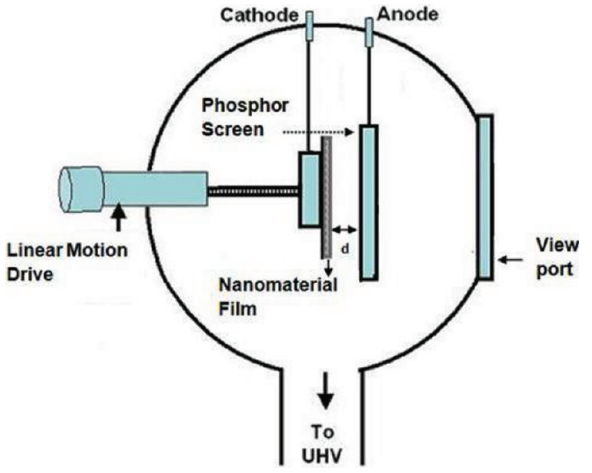

Figure 1. Schematic of field-emission set-up.

EXPERIMENTAL SECTION

Material Synthesis. The growth of branched nanowires heterostructure is carried out in two steps.[19] In brief, the SnO_2 nanowire core, with control over their composition and diameter, was grown using highly pure Sn powder (99.99% pure) in a horizontal tubular furnace at 900 °C in the presence of Ar gas (and 1% O_2) flow.[20] In the second step the as grown SnO_2 nanowires was placed in a thermal evaporation chamber. A W foil of 1 mm thickness and 5 × 1 cm^2 size was mounted between two copper electrodes 2 cm above the SnO_2 nanowires and the chamber was evacuated to 2 × 10^{-5} mbar. The W foil was heated to ~1965 °C by passing current and the depositions were carried out for 30 min. The heating was carried out at two different base pressures viz 9 × 10^{-5} mbar and 7 × 10^{-4} mbar, respectively. The base pressure was varied by inletting air through needle valve. A uniform blue coating was observed on the SnO_2 nanowires after the completion of deposition. No metal catalyst was used and the process relies on the vapor solid process for synthesis of highly pure nanoheterostructures.[1] The morphology of the synthesized product was investigated using SEM and TEM techniques. The crystallographic quality and phase formation (of $WO_{2.72}$) were confirmed by grazing angle XRD measurements.[19]

Field-Emission Studies. The field-emission current density versus applied field ($J-E$) and emission current versus time ($I-t$) measurements were carried in all metal field emission microscope. The field

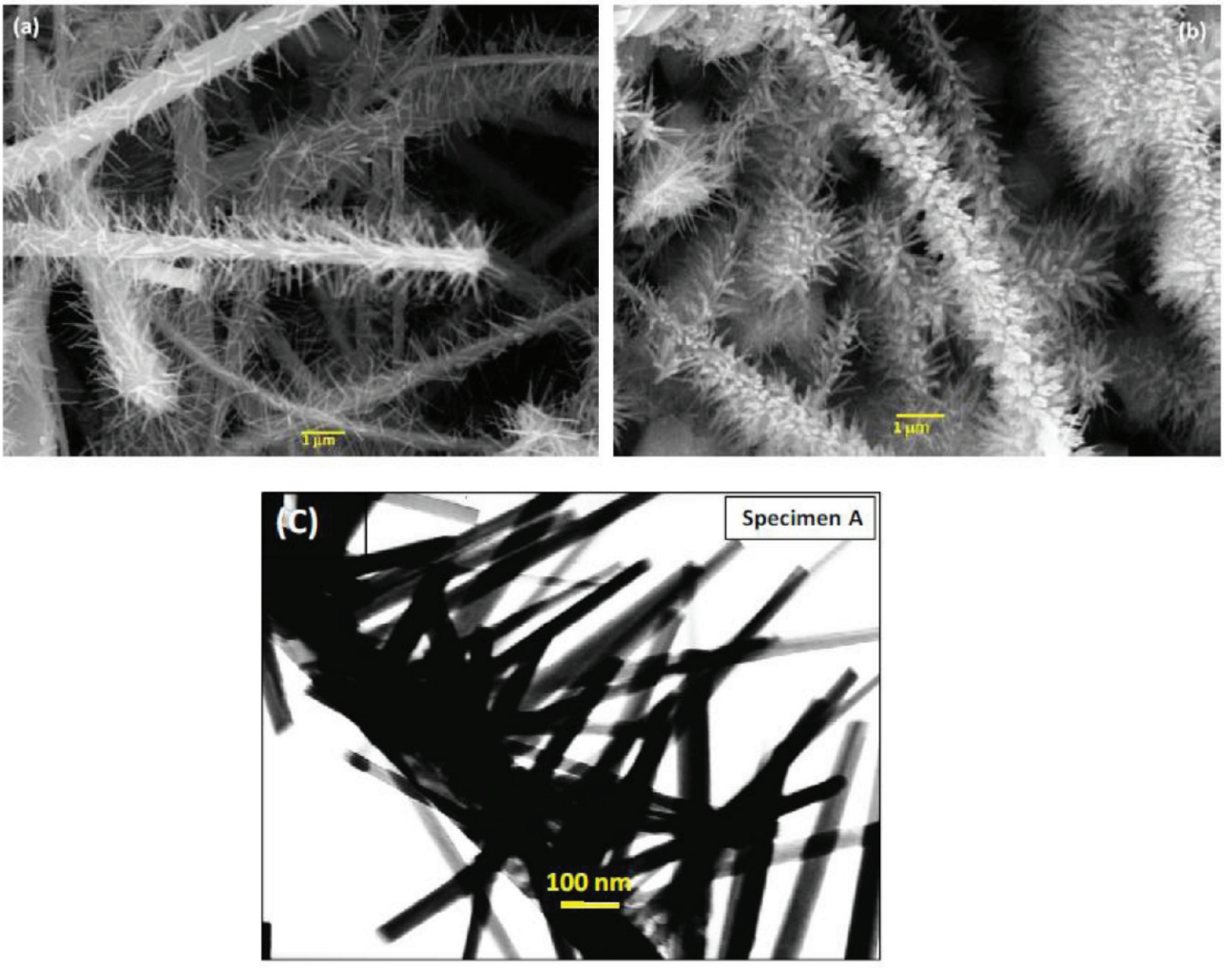

Figure 2. SEM image of SnO_2: $WO_{2.72}$ heterostructures grown at filament temperature of 1965 °C at (a) 9 × 10^{-5} mbar (specimen A) and (b) 7 × 10^{-4} mbar (specimen B) pressure, (c) TEM image of specimen A.

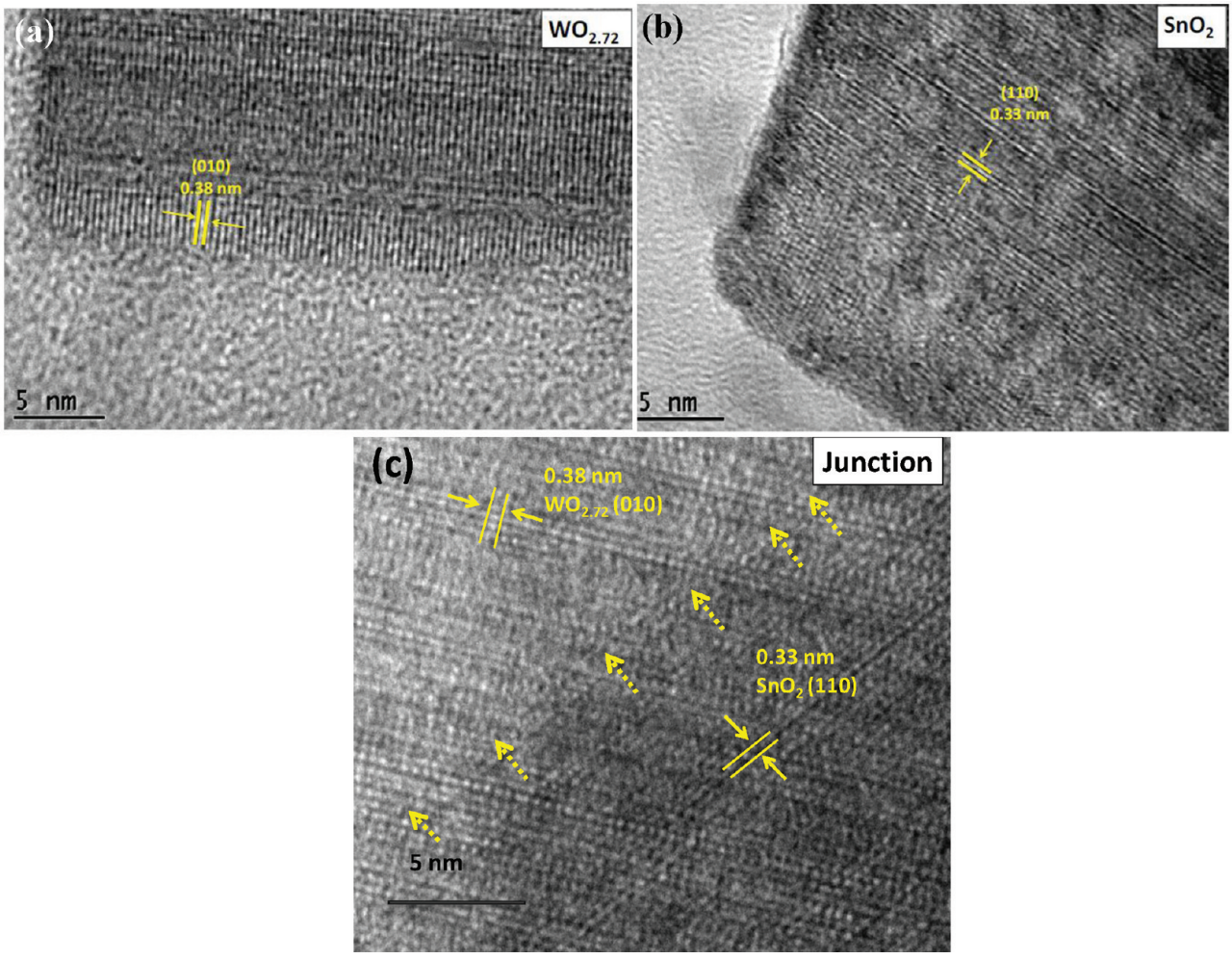

Figure 3. High-resolution TEM images of (a) $WO_{2.72}$ nanothorn, (b) SnO_2 stem, and (c) at the $WO_{2.72}$−SnO_2 junction (dotted arrows indicate the interface between the SnO_2 and $WO_{2.72}$).

emission studies were carried out in a "close proximity" (also termed as "planar diode") configuration, wherein the SnO_2:$WO_{2.72}$ hierarchical nanostructures served as a cathode and a semitransparent cathodoluminescent phosphor screen as an anode. The schematic of field emission setup is shown in Figure.1. We have carried out field-emission studies on two different specimens viz, SnO_2:$WO_{2.72}$ hierarchical nanostructures grown at filament temperature 1965 °C at 9×10^{-5}mbar pressure (specimen A) and at 7×10^{-4}mbar pressure (specimen B), respectively. The as synthesized specimens were pasted onto a copper rod using vacuum compatible conducting silver paste and were held in front of the anode screen at a distance of ∼1 mm. The working chamber was evacuated using ultra high vacuum system comprising turbo molecular pump, a sputter ion pump and a titanium sublimation pump. The cathode (SnO_2:$WO_{2.72}$ hierarchical nanostructures) did not show any appreciable degassing and vacuum could be obtained with usual rate. After baking the system at 150 °C for 8 h, pressure of $\sim 1 \times 10^{-8}$ mbar was obtained. The current density versus applied field (J−E) and the emission current stability (I−t) measurements were carried out at this base pressure using a Keithley 6514 electrometer and a Spellman high voltage DC power supply. Special care was taken to avoid any leakage current by using shielded cables with proper grounding.

RESULTS AND DISCUSSION

The SEM images are shown in the Figure 2. In Figure 2a [Specimen A], $WO_{2.72}$ nanothorns grown at less pressure (9×10^{-5} mbar) on SnO_2 nanowire are of lesser density, smaller diameter (∼50 nm) and larger length (∼1 μm) as compared to Specimen B [Figure.2 (b)]. Specimen B shows higher density of $WO_{2.72}$ nanothorns on the surface of SnO_2 with lesser length and larger diameter (above 100 nm). The change in morphology is dependent on the chamber pressure (oxygen content) during growth. The detailed growth mechanism has been described in our earlier publication.[19] TEM image of Specimen A in Figure 2c shows $WO_{2.72}$ nanothorns with length around 500 nm and tip diameter around 20 nm. Small tip diameter and high aspect ratio of the nanothorns is highly beneficial for field-emission applications.

HRTEM images shown in Figure 3. confirm the high crystalline nature of the nanowires. Images a and b in Figure 3 shows the lattice image of $WO_{2.72}$ nanothorn and SnO_2 nanowire respectively with uniform lattice spacing throughout the structure. The $WO_{2.72}$ nanothorns are found to grow along (010) direction. Figure 3c. shows the HRTEM image at the interface of the SnO_2 and $WO_{2.72}$ nanothorn. A sharp interface between the two structures is visible (as indicated by the dotted arrows in the Figure) with $WO_{2.72}$ nanothorn branches self-assembled at some angle on the SnO_2 nanowire stem.

SEM and TEM observations of the SnO_2:$WO_{2.72}$ heterostructures expects them to show good field emission properties.

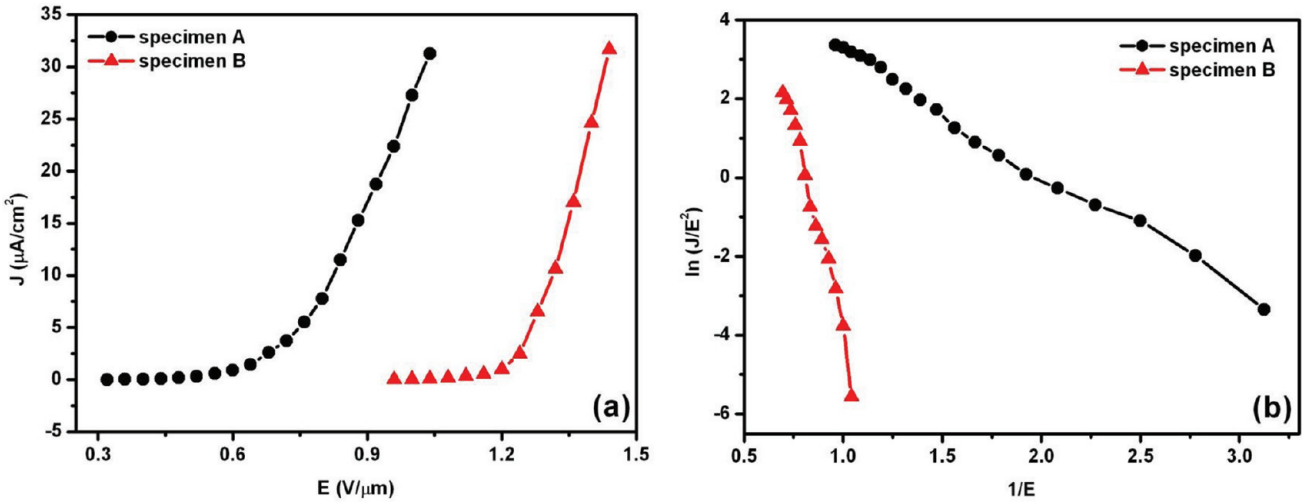

Figure 4. Field emission from SnO_2:$WO_{2.72}$ heterostructures. (a) Field-emission current density−applied electric field (J−E) characteristics. (b) Corresponding Fowler−Nordheim (F−N) plot.

Table 1. Synthesis Method and Turn-on Field of SnO_2, WO_3 and Nano-heterostructures Field Emitters

emitter	synthesis method	turn-on field (V μm^{-1}) (J = 10 $\mu A/cm^2$)	ref
W nanothorn arrays on WO_3 nanowhiskers	two-step evaporation	6.2	8
In_2O_3 nanowire decorated Ga_2O_3 nanobelt heterostructures	thermal evaporation	1.31	21
ZnS nanotubes−In nanowire core−shell heterostructures	thermal evaporation	5.43	22
$W_{18}O_{49}$ nanotip arrays	two-step evaporation	2.0	23
$WO_{3-\delta}$ nanowire network	thermal evaporation	13.85	24
SnO_2 nanowhiskers	thermal evaporation	1.37 (0.1 $\mu A/cm^2$)	25
SnO_2 nanowires	thermal evaporation	1.3 (1 $\mu A/cm^2$)	26
SnO2:$WO_{2.72}$ nanowire heterostructures	two-step evaporation	0.82	present study

The present field-emission study is analogous to our previous field-emission study of the $WO_{2.72}$ nanowires.[11]

The field-emission current density-applied field (J−E) characteristic of the SnO_2:$WO_{2.72}$ heterostructures is depicted in Figure 4a. The turn-on field, defined as the field required to draw an emission current of density ∼10 $\mu A/cm^2$, is found to be ∼0.82 and 1.38 V/μm for specimen A and B, respectively. As the applied voltage was increased further, the emission current was found to increase very rapidly and an emission current density of ∼31 $\mu A/cm^2$ has been drawn at an applied field of ∼1.04 and 1.92 V/μm for specimen A and B, respectively. Reports mentioning the exploration of the SnO_2:$WO_{2.72}$ heterostructures as field emitter are not available; however, for comparison, the present results are weighed against the field-emission properties of pure SnO_2 nanostructures, pure WO_x nanostructures and other heteronanostructures in the literature.[21−26] The results are summarized in table of comparison (Table 1).

The ultralow value of the observed turn-on field for specimen A is due to the high aspect ratio as compared to specimen B. Also, higher density of $WO_{2.72}$ nanothorns in specimen B causes more electric field screening, which results in higher turn on field as compared to specimen A. M. Furubayashi et al.[27] investigated the effect of the degree of dispersion of tungsten oxide nanowires on their field-emission properties and concluded that the electric field becomes stronger as the emitter pitch becomes wider. In our case, the emitter pitch for specimen A is quite wider than that of specimen B and hence the electric field experience by an individual $WO_{2.72}$ nanothorn in specimen A is higher and accordingly shows lower turn-on field. The applied field E is defined as $E = V/d$, where V is the applied voltage and d is separation between the emitter cathode and the anode. This field is also referred as an average field. In the present case, the current density J is estimated by considering the entire area of the emitter (0.3 cm^2).

The possible reason for the enhancement of the electric field in SnO_2:$WO_{2.72}$ hierarchical heterostructures can be explained on the basis of U. K. Gautam et al.'s report on ZnS nanotubes−In nanowire core−shell heterostructures.[22] First, the primary applied field would be enhanced by a stem structure (SnO_2 nanowires in our case), which acts as a substrate for the secondary branches ($WO_{2.72}$). A stronger field at the bottom of the branches is equivalent to an effectively higher applied bias, which then in turn is further enhanced by the 1D branch. Furthermore, in our case, most of the emission is from $WO_{2.72}$ nanothorn branches, which has higher aspect ratio as well as widely spread over the entire SnO_2 stem in specimen A as compare to the other nanoheterostructures reported earlier.[8,21,22]

The Fowler−Nordheim (F−N) plot, i.e., ln (J/E^2) versus ($1/E$), derived from the observed J−E characteristic is shown in Figure.4 (b). The F−N plot shows overall linear behavior with decrease in the slope (nonlinearity) in very high applied field range. Such type of F−N plot exhibiting tendency toward nonlinearity at

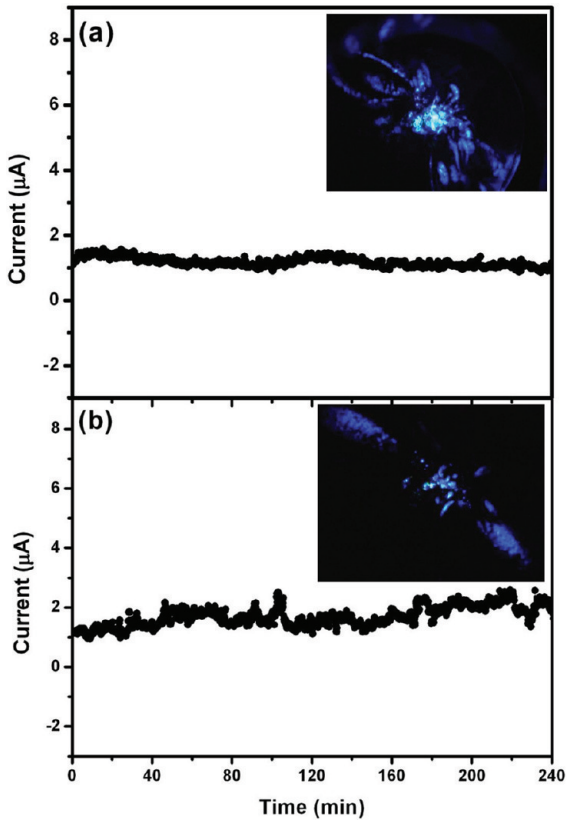

Figure 5. Field-emission current stability ($I-t$) and field-emission micrographs (inset) of SnO_2:$WO_{2.72}$ heterostructures (a) specimen A and (b) specimen B.

very high applied field has been reported for $WO_{2.72}$ in our previous work.[11]

For field-emission electron sources, along with the emission competence, the current stability is also a decisive and an important parameter. $I-t$ plot of Specimen A and B recorded at the base pressure of 1×10^{-8} mbar at the preset current value of $\sim 1\ \mu$A (at applied voltages of $\sim$0.5 kV, $\sim$ 1.4 kV for specimen A and B) over the duration of four hours is shown in Figure 5a, b. As shown in Figure 5a, the emission current is almost steady for specimen A, whereas in specimen B, i.e., Figure 5b the instability in the emission current is seen. This can be attributed to the adsorption, desorption of residual gas molecules present in the ambient of the specimen, and the phenomenon of ion bombardment during emission process. Specimen B may not withstand to large field, which is significantly seen in the form of the fluctuations. In specimen A, the $WO_{2.72}$ nanothorns are well-separated from each other and have a small diameter, whereas in specimen B, nanothorns are densely crowded which causes more surface area for the adsorption and diffusion of residual gas molecules on the emitter surface to occur. The fluctuations are in the form of "spikes", such as digital pulse. The emitter surface would become cleaner because of the ion bombardment induced desorption of the residual gases, and the clean surface thus produced leads to stabilization of the emission current at a higher value.[28] The striking feature of the field-emission behavior of specimen A is that the average emission current remains nearly constant over the entire duration and shows no signs of degradation. This is very important feature, particularly from the practical application of the emitter material as an electron source.

CONCLUSIONS

In summary, the field-emission properties of $WO_{2.72}$ nanothorns grown on SnO_2 nanowires were investigated. The turn-on field is found to be $\sim$0.82 V/μm for $WO_{2.72}$ nanothorns deposited at 9×10^{-5} mbar pressure. An emission current density of $\sim 31\ \mu A/cm^2$ was recorded at an applied field of $\sim$1.04 V/μm for this specimen. The enhancement in the field-emission characteristic is attributed to the special geometry of the heteronanostructures. The results show SnO_2:$WO_{2.72}$ nanowire heterostructures are promising candidate for application in field-emission devices.

AUTHOR INFORMATION

Corresponding Author

*E-mail: shash@barc.gov.in (S.S.); mam@physics.unipune.ac.in (M.A.M.).

ACKNOWLEDGMENT

D.R.S. is thankful to DRDO and Director MTRDC, Bangalore, for financial support. P.G.C. is thankful to the UGC, India, for the award of Rajiv Gandhi National Fellowship. D.S.J. thanks C.SIR for Emeritus Scientist scheme.

REFERENCES

(1) Barth, S.; Hernandez-Ramirez, F.; Holmes, J. D.; Romano-Rodriguez, A. *Prog. Mater. Sci.* **2010**, *55*, 563.
(2) Comini, E.; Baratto, C.; Faglia, G.; Ferroni, M.; Vomiero, A.; Sberveglieri, G. *Prog. Mater. Sci.* **2010**, *55*, 563.
(3) Lao, J. U.; Wen, J. G.; Ren, Z. F. *Nano Lett.* **2002**, *2*, 1287.
(4) Bae, S. Y.; Seo, H. W.; Choi, H. C.; Park, J. *J. Phys. Chem. B* **2004**, *108*, 12318.
(5) Ye, C.; Zhang, L.; Fang, X.; Wang, Y.; Yan, P.; Zhao, L. *Adv. Mater.* **2004**, *16*, 1019.
(6) Hu, J.; Bando, Y.; Zhan, J.; Yuan, X.; Sekiguchi, T.; Golberg, D. *Adv. Mater.* **2005**, *17*, 971.
(7) Milliron, D. J.; Hughes, S. M.; Cui, Y.; Manna, L.; Li, J.; Wang, L.; Alivisatos, A. P. *Nature* **2004**, *430*, 190.
(8) Baek, Y.; Song, Y.; Yong, K. *Adv. Mater.* **2006**, *18*, 3105.
(9) Zhou, J.; Gong, L.; Deng, S. Z.; Chen, J.; She, J. C.; Xu, N. S. *Appl. Phys. Lett.* **2005**, *87*, 223108.
(10) Yue, S.; Pan, H.; Ning, Z.; Yin, J.; Wang, Z.; Zhang, G. *Nanotechnology* **2011**, *22*, 115703.
(11) Late, D. J.; Kashid, R. V.; Rout, C. S.; More, M. A.; Joag, D. S. *Appl. Phys. A: Mater. Sci. Prog.* **2009**, *98*, 751.
(12) Bhise, A. B.; Late, D. J.; Ramgir, N. S.; More, M. A.; Mulla, I. S.; Pillai, V. K.; Joag, D. S. *Appl. Surf. Sci.* **2007**, *253*, 9159.
(13) Bhise, A. B.; Late, D. J.; Sathe, B.; More, M. A.; Mulla, I. S.; Pillai, V. K.; Joag, D. S. *J. Exp. Nanosci.* **2010**, *5*, 527.
(14) Bhise, A. B.; Late, D. J.; Walke, P. S.; More, M. A.; Pillai, V. K.; Mulla, I. S.; Joag, D. S. *J. Cryst. Growth* **2007**, *307*, 87.
(15) Mathur, S.; Barth, S. *Small* **2007**, *3*, 2070.
(16) Zhang, D. F.; Sun, L. D.; Jia, C. J.; Yan, Z. G.; You, L. P.; Yan, C. H. *J. Am. Chem. Soc.* **2005**, *127*, 13492.
(17) Vomiero, A.; Ferroni, M.; Comini, E.; Faglia, G.; Sberveglieri, G. *Nano Lett.* **2007**, *7*, 3553.
(18) Sun, S.; Meng, G.; Zhang, G.; Zhang, L. *Cryst. Growth Des.* **2007**, *7*, 1988.
(19) Sen, S.; Kanitkar, P.; Sharma, A.; Muthe, K. P.; Rath, A.; Deshpande, S. K.; Kaur, M.; Aiyer, R. C.; Gupta, S. K.; Yakhmi, J. V. *Sens. Actuators, B* **2010**, *147*, 453.
(20) Kumar, V.; Sen, S.; Muthe, K. P.; Gaur, N. K.; Gupta, S. K.; Yakhmi, J. V. *Sens. Actuators, B* **2009**, *138*, 587.
(21) Lin, J.; Haung, Y.; Bando, Y.; Tang, C.; Li, C.; Golberg, D. *ACS Nano* **2010**, *4*, 587.

(22) Gautam, U. K.; Fang, X.; Bando, Y.; Zhan, J.; Golberg, D. *ACS Nano* **2008**, *2*, 1015.
(23) Zhou, J.; Gong, L.; Deng, S. Z.; Chen, J.; She, J. C.; Xu, N. S. *Appl. Phys. Lett.* **2005**, *87*, 223108.
(24) Zhou, J.; Ding, Y.; Deng, S. Z.; Gong, L.; Xu, N. S.; Wang, Z. L. *Adv. Mater.* **2005**, *17*, 2107.
(25) Luo, S. H.; Wan, Q.; Liu, W. L.; Zhang, M.; Di, Z. F.; Wang, S. Y.; Song, Z. T.; Lin, C. L.; Dai, J. Y. *Nanotechnology* **2004**, *15*, 1424.
(26) Wang, L.; Lin, J.; Yun, Y.; Guo, T. *Phys. Status Solidi C* **2011**, DOI: 10.1002/pssc.201084167.
(27) Furubayashi, M.; Nagota, K.; Moritani, H.; Hamaguchi, T.; Nakao, M. *Micoelectron. Eng.* **2010**, *87*, 1594.
(28) Panda, S. K.; Datta, A.; Sinha, G.; Chaudhuri, S.; Chavan, P. G.; Patil, S. S.; More, M. A.; Joag, D. S. *J. Phys. Chem. C* **2008**, *112*, 6240.